ELSEVIER

Journal of Power Sources 114 (2003) 10–14

JOURNAL OF POWER SOURCES

www.elsevier.com/locate/jpowsour

Impedance studies on mesocarbon microbeads supported Pt-Ru catalytic anode

Yi-Cheng Liu, Xin-Ping Qiu*, Wen-Tao Zhu, Guo-Shi Wu

Department of Chemistry, Tsinghua University, Beijing 100084, PR China

Received 15 February 2002; received in revised form 5 August 2002; accepted 25 September 2002

Abstract

The impedance behaviors of direct methanol fuel cell anode using mesocarbon microbeads supported Pt-Ru catalysts were studied. A loop reflecting an inductive behavior appears at the low-frequency end only when the anode is at higher overpotential. The Nafion content in the catalyst, the MEA hot press condition and the effects of the cell temperature on the impedance behaviors of the anode electrode were also investigated.

Keywords: Direct methanol fuel cell; Impedance spectroscopy; Methanol oxidation

1. Introduction

Recently, direct methanol fuel cells (DMFCs) have been receiving increasing attention for the advantages of ease transportation and storage of the fuel, high-energy efficiency, simplicity and convenience. However, DMFCs are also faced with a number of technical challenges: methanol crossover and slow anode kinetics [1,2].

A number of different approaches are being investigated to improve anode kinetics. The greatest effort is being directed toward the development of more active electrocatalysts: binary to quaternary platinum alloys [3–10]. Other approaches for dealing with slow anode kinetics involve increased cell temperature and pressure [11]. However, there have a little work for dealing with the structure of the anode catalysts to improve the mass transport of the fuel.

In the present work, a new Pt-Ru anode catalyst with mesocarbon microbeads (MCMB) as the support was investigated. Mesocarbon microbeads derived from petroleum residua is a kind of micron carbon particles, which may be favorite for mass transport during the electro-catalytic reaction occurs. Anode characterization by ac impedance was performed using a procedure similar to the one discussed in [12,13]. The Faradaic impedance of DMFC anodes operating without mass-transport limitations was investigated. The variation of the performance of the anode was investigated with respect to Nafion content of the catalyst, pressure of hot press, and cell temperature.

2. Experimental

2.1. Preparation of mesocarbon microbeads supported Pt-Ru catalysts

MCMBs (Shanshan Inc., Shanghai, PR China) were boiled in 2 M KOH solutions boiling for 1 h before the supported catalyst preparation. The supported catalysts were prepared by liquid-phase reduction of chloroplatinic acid and ruthenium chloride with sodium hyposulfite. MCMB (3.7 g) was suspended in 200 ml of water at 80 °C. An aqueous solution (50 ml) containing 1 g chloroplatinic acid and appropriate amount of ruthenium chloride solution (Pt:Ru molar ratio is 3:1) were added slowly to the MCMB suspension and allowed for complete impregnation (lasting over 1 h). Then, 50 ml of 0.5 M $Na_2S_2O_4$ was added drop by drop. The resultant mixture was maintained at 80 °C for 3 h to allow complete reduction of Pt and precipitation of metallic oxides. Subsequently, the mixture was filtered, and washed copiously with hot distilled water to remove chloride ions. The catalyst was dried in an air oven at 80 °C for 5 h, and was heat-treated at 300 °C for 1 h.

* Corresponding author. Tel.: +86-10-627-94235; fax: +86-10-627-94234.
E-mail address: qiuxp@mail.tsinghua.edu.cn (X.-P. Qiu).

0378-7753/02/$ – see front matter
PII: S0378-7753(02)00527-X

2.2. Procedure to measure anode impedances

The experimental set-up and the procedure to measure DMFC anode impedances have been earlier described in detail [12]. In short, impedance measurements were conducted on a cell consisting of a Pt-Ru/MCMB anode (Pt loading: 0.3 mg cm^{-2}), a Nafion membrane, and a Pt/C (E-TEK, Pt loading: 1 mg cm^{-2}) cathode sandwiched between two conventional graphite flow field plates. The anode was supplied with 1.0 M methanol solutions by using very high fuel flow rates (10 times the stoichiometric rates). The cathode was operated on hydrogen, which served as a dynamic hydrogen electrode (DHE). All anode impedance spectra reported here were measured between anode and DHE in the complete fuel cell. The frequency generator analyzer was an Schlumberger Solartron FRA 1255 controlled by a personal computer and coupled to a potentiostat instrument (Solartron 1287) that allows modulation of large dc currents. Impedance spectra were usually obtained at frequencies between 10 kHz and 0.5 Hz with 10–15 steps per decade. The integration time was set at 10 s. The amplitude of the sinusoidal potential signal was 10 mV.

3. Results and discussion

3.1. Model of methanol electro-oxidation

Depending on the DMFC anode potential (versus DHE), its impedance plots can have different features. Figs. 1 and 2 show a series of Nyquist plots of two supported Pt-Ru anodes working with various overpotentials. The Pt-Ru/MCMB electrode and Pt-Ru/C (E-TEK) electrode were prepared and measured at the same method. The Pt loading is ca. 0.3 mg cm^{-2} in each electrode. Both anodes show the equivalent results. The ac spectra show small potential independent impedance in the high frequency region (10–10000 Hz), which is superimposed to a lower frequency arc that has a magnitude dependent on potential. Some similar phenomena had been reported in the proton exchange

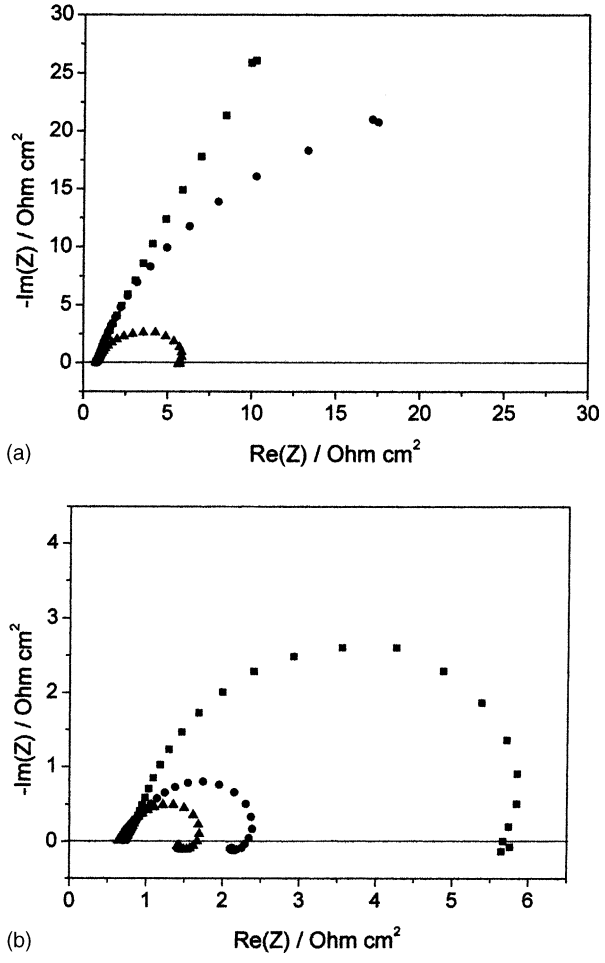

Fig. 1. Pt-Ru/MCMB anode impedance plots at different potential (vs. DHE). (a) (■) 0.1 V, (●) 0.2 V, (▲) 0.3 V; (b) (■) 0.3 V, (●) 0.4 V, (▲) 0.5 V. Methanol concentration: 1.0 M; cell temperature: 90 °C; Pt loading: 0.3 mg cm^{-2}.

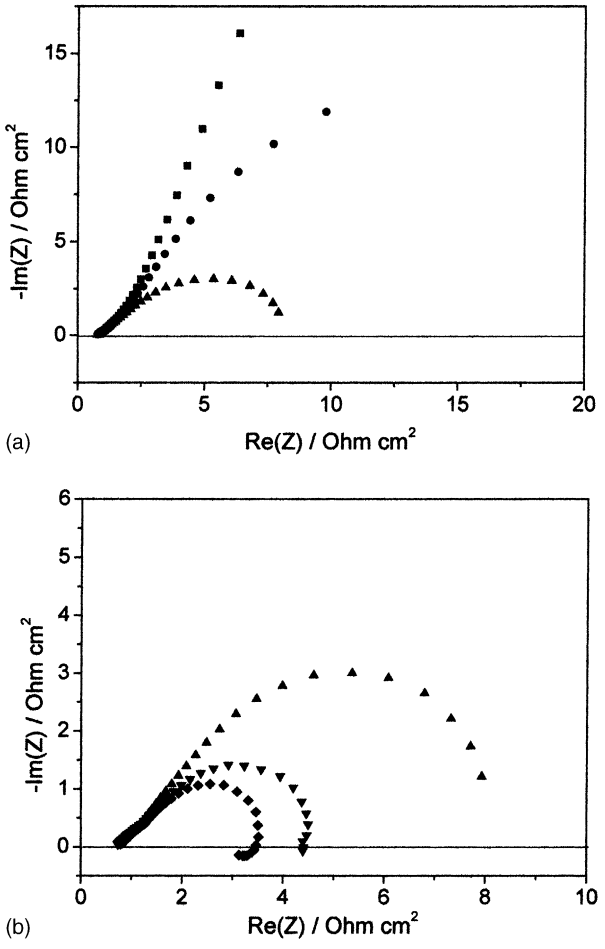

Fig. 2. Pt-Ru/C anode (E-TEK) impedance plots at different potential (vs. DHE). (a) (■) 0.1 V, (●) 0.2 V, (▲) 0.3 V; (b) (▲) 0.3 V, (▼) 0.4 V, (◆) 0.5 V. Methanol concentration: 1.0 M; cell temperature: 90 °C; Pt loading: 0.3 mg cm^{-2}.

membrane fuel cells (PEMFCs). It was reported that the impedance arc shrinks with the decease of cell potential for H_2/O_2 polymer electrolyte fuel cells (PEFCs) [14,15], which was regarded to be related to the charge transfer resistance of the oxygen reduction reaction.

A loop reflecting an inductive behavior appears at the low-frequency end when the potential is larger than 0.3 V (versus DHE). The loop had been reported in the research of Müller et al. [13]. It is clear that increasing overpotential is helpful for the methanol oxidation. Therefore, the formation of the loops is due to the improvement of methanol electro-oxidation kinetics.

The inductive behavior had been explained by Müller et al. [13] using the kinetic theory derived by Harrington and Conway [16] for reactions involving intermediate adsorbates:

$$CH_3OH \rightarrow (CO)_{ads} \rightarrow CO_2 \quad (1)$$

When it is assumed that mass transport limitations do not occur, the Faradaic impedance can be expressed as (the full derivation is given in [16])

$$Z = \frac{1}{A} + \frac{j\omega + C}{B} = \left(\frac{1}{R_\infty} + \frac{1}{R_0 + j\omega L}\right)^{-1}$$

where $R_\infty = 1/A$; $R_0 = C/B$; $L = 1/B$.

A, B, C are the auxiliary parameter, defined as

$$A = F\left(\frac{\partial r_e}{\partial E}\right)_\theta, \qquad B = \frac{F^2}{q_{CO}}\left(\frac{\partial r_e}{\partial \theta}\right)_E \left(\frac{\partial r_{CO}}{\partial E}\right)_\theta,$$

$$C = \frac{-F}{q_{CO}}\left(\frac{\partial r_{CO}}{\partial \theta}\right)_E$$

where r_e is the net rate of production of electrons, r_{CO} the net rate of production of $(CO)_{ads}$, θ the fractional surface coverage of CO, and q_{CO} the charge required for adsorption of CO to complete coverage.

This expression for the Faradaic impedance leads to the equivalent circuit shown in Fig. 3. When it is used to model the impedance behavior of the DMFC anode, the resulting shape of the Nyquist plots agrees well with the experimentally observed plots (Fig. 4). The distortion of the spectrum is also observed [13] and believed to be the roughness of the catalytic layer [17], or a current constriction effect [18]. The inductance L which means the current signal follows a voltage perturbation with a phase delay is due to slowness

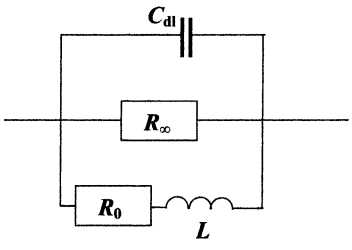

Fig. 3. Equivalent circuit for modeling the Faradaic impedance of DMFC anodes.

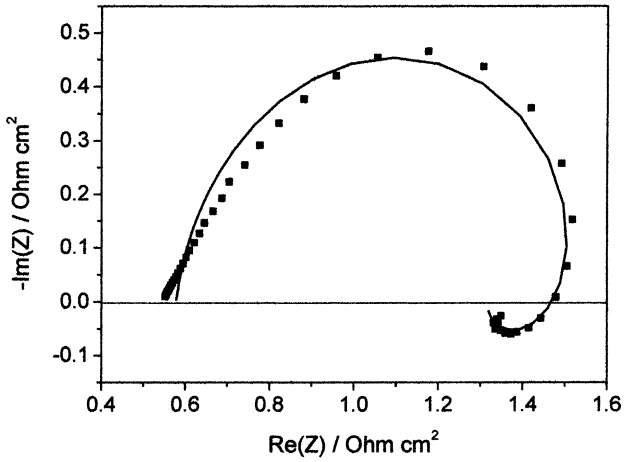

Fig. 4. Modeling of the Faradaic impedance of a Pt-Ru/MCMB anode at 0.5 V (vs. DHE). Methanol concentration: 1.0 M; cell temperature: 90 °C. Dot: measured spectrum, solid line: simulated spectrum using equivalent circuit of Fig. 3 and fitting of parameters: $C_{dl} = 0.0062$ F cm^{-2}; $R_\infty = 0.94\ \Omega$ cm^2; $R_0 = 3.06\ \Omega$ cm^2; $L = 0.20$ H cm^{-2}.

of $(CO)_{ads}$ coverage relaxation. R_0 serves to modify the phase-delay according to the reaction scheme, and the R_∞ arm of the circuit is associated with the part of the current response, which occurs without change in coverage [16].

3.2. Effect of cell temperature and process parameter on the anode performance

It can be obtained from Figs. 1 and 2 that anode potentials have great influence on the impedance plots. Therefore, in order to study the effect of operating conditions and process parameter on the anode impedance, all the anode potential of the experiment below were set to 0.5 V (versus DHE).

Fig. 5 shows Pt-Ru/MCMB anode impedance plots at different cell temperature when supplied with 1 M aqueous

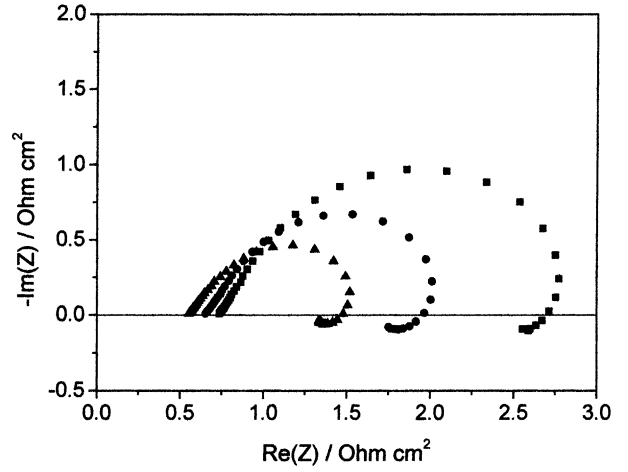

Fig. 5. Pt-Ru/MCMB anode impedance plots at different cell temperature. Anode potential: 0.5 V (vs. DHE); methanol concentration: 1.0 M, Pt loading: 0.3 mg cm^{-2}. Cell temperature: (■) 60 °C; (●) 75 °C; (▲) 90 °C.

Table 1
Comparison of fitting parameters using equivalent circuit of Fig. 3 at various cell temperatures and process parameters

Temperature (°C)	Nafion content (%)	Pressure of hot press (MPa)	C_{dl} (F cm^{-2})	R_∞ (Ω cm^2)	R_0 (Ω cm^2)	L (H cm^{-2})
60	10	7.5	0.0085	1.97	7.28	2.67
75	10	7.5	0.0072	1.35	3.66	0.40
90	10	7.5	0.0062	0.94	3.06	0.20
90	5	7.5	0.0053	1.18	2.87	0.35
90	20	7.5	0.0034	1.58	2.83	0.22
90	10	5	0.0028	1.24	2.55	0.21
90	10	10	–	–	–	–

methanol solution. The fitting parameters using equivalent circuit of Fig. 3 are shown in the Table 1. The simulated spectrums are not presented in the figure for clarity. The intercepts on the real axis at the high frequency decease with the increase of cell temperature. The arc occurring at the medium-frequency shrinks greatly in diameter when the cell temperature is raised, and this is corresponding to the decrease of R_∞ (from 1.97 Ω cm^2 at 60 °C to 0.94 Ω cm^2 at 90 °C). The inductance L also decreased with cell temperature increase (from 2.67 H cm^{-2} at 60 °C to 0.20 H cm^{-2} at 90 °C). This may be due to the new steady-state coverage of $(CO)_{ads}$ after a potential perturbation is easier to be established at higher temperature according to the postulate of slowness of $(CO)_{ads}$ coverage relaxation [13].

Fig. 6 shows Pt-Ru/MCMB anode impedance plots with various Nafion content in the catalyst layer when supplied with 1 M aqueous methanol solution at 90 °C. All the anodes were prepared and measured at the same condition except the Nafion content in the catalyst layer. The Fitting parameters using equivalent circuit of Fig. 3 are also shown in the Table 1. The anode of containing 10 wt.% Nafion in the catalyst ink shows the smaller arc and smaller inductance L than that of the other two anodes.

Past studies on the influence of Nafion loading on PEFC performance revealed that there was an optimal amount of the Nafion ionomer in the catalyst layer in the case of the carbon-supported platinum, and the optimal amount should depend on the Pt catalyst loading in the catalyst layer [19,20]. The smallest arc of the PEFC impedance was obtained with the optimized Nafion content (0.8 mg cm^{-2} ionomer with Pt loading: 0.4 mg cm^{-2}), which the cell showed the best performance [15]. This result is similar with the results showed in Fig. 6. The specific protonic conductivity of a catalyst layer prepared with recast Nafion^{TM} is proportional to the volume fraction of Nafion in the catalyst layer [21]. The increase of the arc diameter at the highest Nafion content in the catalyst layer was due to a resistance of mass transport with an increase of a thickness of ionomer on the Pt particles. Therefore, it is important to optimize Nafion content in the catalyst layer.

Fig. 7 shows DMFC anode impedance plots at various pressures of hot press of MEA. The MEA was obtained by hot-pressing the anode and cathode on either side of a pre-treated Nafion-112^{TM} membrane under a selected pressure at 130 °C for 3 min. All the anodes were measured at the same condition except the pressure of hot press. The Fitting parameters using equivalent circuit of Fig. 3 are also shown

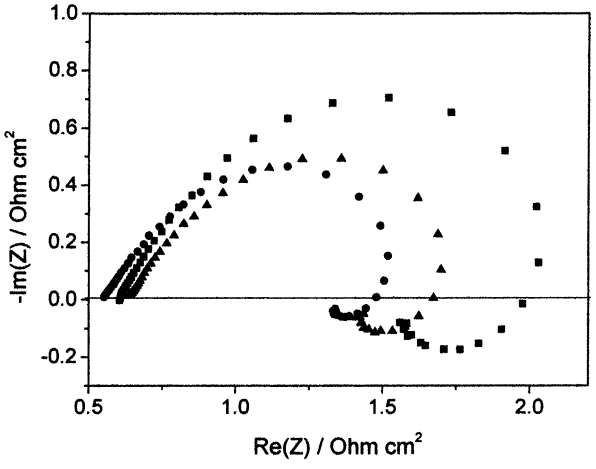

Fig. 6. DMFC anode impedance plots with various Nafion content in the catalyst layer. Anode potential: 0.5 V (vs. DHE); cell temperature: 90 °C; methanol concentration: 1.0 M; Pt loading: 0.3 mg cm^{-2}. Nafion content: (■) 5 wt.%; (●) 10 wt.%; (▲) 20 wt.%.

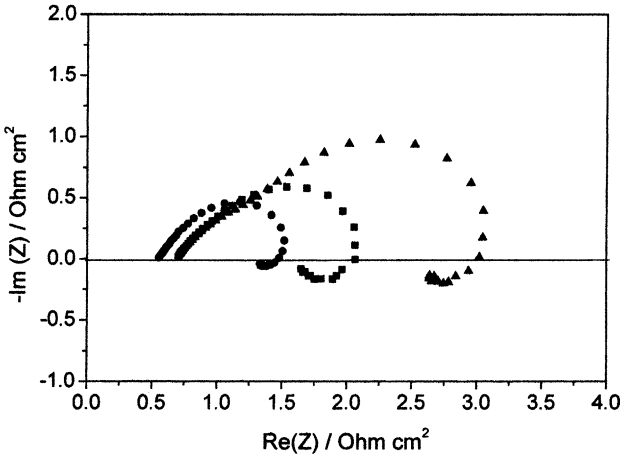

Fig. 7. DMFC anode impedance plots at various pressure of hot press of MEA. Anode potential: 0.5 V (vs. DHE); cell temperature: 90 °C; methanol concentration: 1.0 M; Nafion content: 10 wt.%. Pressure: (■) 5.0 MPa; (●) 7.5 MPa; (▲) 10.0 MPa.

in the Table 1. The anode of which hot pressed at 7.5 MPa shows the smaller arc and smaller inductance than that of the anodes which was hot pressed at 5.0 MPa. The plot of the anode hot pressed at 10 MPa shows a different feature. A high frequency arc occurred and followed a large medium frequency arc and a loop at the low frequency end. The result indicates that the equivalent circuit shown in Fig. 3 is not suitable for explanation of the plot, which may be due to the mass transport limitations could not be eliminated even by using very high fuel flow rates (10 times the stoichiometric rate) when the anode hot pressed at 10 MPa.

The results indicate that the process parameter of hot press should be considered carefully. Light pressure (5 MPa) may cause the contact of the electrodes and the membrane not well; but heavy pressure (10 MPa) will make the contact of the electrodes and the membrane extremely tight to block the methanol transport and hinder the CO_2 removal.

It should be pointed that there exists a distinct difference in the parameter-fitting result of capacitor C_{dl} between our research and the research of Müller et al. [13]. The magnitude of the capacitance in Müller's study is in the order of 0.1–1 F cm^{-2}, which is too high to be explained by double-layer capacitance. Instead, it is believed to be associated with the redistribution of charge at the anode. But all of the magnitude of the capacitance in our research work is in the order of 0.001–0.01 F cm^{-2}, depending on parameters such as cell temperature, Nafion content in the catalyst layer and so on. This result is suit for the double-layer capacitances of the DMFC anode and cathode, as reported by the other researchers [22,23]. The reason for this difference of the capacitance has to be clarified.

4. Conclusion

The impedance behaviors of DMFC anode using MCMB supported Pt-Ru catalysts were studied without mass-transport limitations. A loop reflecting an inductive behavior appears at the low-frequency end only when the anode is at higher overpotential. A simple equivalent circuit was used to explain the characteristic inductive behavior of the DMFC anode. The insight study of cell temperature, Nafion content in the catalyst layer and the pressure of hot press of anode on the character of methanol electro-oxidation was obtained according to the change of fitting parameters of the equivalent circuit. The anode with appropriate Nafion content (10 wt.%) and pressure (7.5 MPa) of hot press shows the best performance at high cell temperature.

References

[1] S. Wasmus, A. Küver, J. Electroanal. Chem. 461 (1999) 14.
[2] A. Heinzel, V.M. Barragan, J. Power Sources 84 (1999) 70.
[3] M. Watanabe, M. Uchida, S. Motoo, J. Electroanal. Chem. 229 (1987) 395.
[4] B. Beden, F. Kadirgan, C. Lamy, J.M. Leger, J. Electroanal. Chem. 127 (1981) 75.
[5] G. Gökağac, B.J. Kennedy, J.D. Cashion, L.J. Brown, J. Chem. Soc., Faraday Trans. 89 (1993) 151.
[6] A.S. Aricò, H. Kim, A.K. Shukla, M.K. Ravikumar, V. Antonucci, N. Giordano, Electrochim Acta 39 (1994) 691.
[7] H.M. Saffarian, R. Srinivasan, D. Chu, S. Gilman, Electrochim. Acta 43 (1998) 1447.
[8] A.K. Shukla, M.K. Ravikumar, A.S. Aricò, G. Candiano, V. Antonucci, N. Giordano, J. Appl. Electrochem. 25 (1995) 528.
[9] P.K. Shen, A.C.C. Tseung, J. Electrochem. Soc. 141 (1994) 3082.
[10] A.S. Aricò, Z. Poltarzewski, H. Kim, A. Morana, N. Giordano, V. Antonucci, J. Power Sources 55 (1995) 159.
[11] A.S. Aricò, P. Creti, P.L. Antonucci, J. Cho, H. Kim, V. Antonucci, Electrochim. Acta 43 (1998) 3719.
[12] J.T. Müller, P.M. Urban, J. Power Sources 75 (1998) 139.
[13] J.T. Müller, P.M. Urban, W.F. Hölderrich, J. Power Sources 84 (1999) 157.
[14] V.A. Paganin, C.L.F. Oliveira, E.A. Ticianelli, T.E. Springer, E.R. Gonzalez, Electrochim. Acta 43 (1998) 3761.
[15] J.M. Song, S.Y. Cha, W.M. Lee, J. Power Sources 94 (2001) 78.
[16] D.A. Harrington, B.E. Conway, Electrochim. Acta 32 (1987) 1703.
[17] A. Maritan, Electrochim. Acta 35 (1990) 141.
[18] S. Ahn, B.J. Tatarchuk, J. Electrochem. Soc. 142 (1995) 4169.
[19] E.A. Ticianelli, C.R. Derouin, A. Redondo, S. Srinivasan, J. Electrochem. Soc. 135 (1988) 2209.
[20] V.A. Paganin, E.A. Ticianelli, E.R. Gonzalez, J. Appl. Electrochem. 26 (1996) 297.
[21] C. Boyer, S. Gamburzev, O. Velev, S. Srinivasan, A.J. Appleby, Electrochim. Acta 43 (1998) 3703.
[22] J. Fleig, J. Maier, J. Electrochem. Soc. 144 (1997) L302.
[23] T.E. Springer, T.A. Zawodzinski, M.S. Wilson, S. Gottesfeld, J. Electrochem. Soc. 143 (1996) 587.